

Synthesis of zeolite LTA from thermally treated kaolinite

Síntesis de zeolita LTA a partir de caolinita tratada térmicamente

Carlos Alberto Ríos Reyes^{1}, Craig Denver Williams², Oscar Mauricio Castellanos Alarcón³*

¹ Escuela de Geología, Universidad Industrial de Santander, Ciudad Universitaria Carrera 27 Calle 9, A.A. 678, Bucaramanga, Colombia.

² University of Wolverhampton, Wulfruna Street, Wolverhampton WV1 1SB, England.

³ Programa de Geología, Universidad de Pamplona, Calle 107 N.º. 103-51, Pamplona, Colombia.

(Recibido el 29 de septiembre de 2009. Aceptado el 25 de febrero de 2010)

Abstract

X-ray diffraction, scanning electron microscopy, Fourier transform infrared spectroscopy, ²⁹Si and ²⁷Al nuclear magnetic resonance and thermogravimetric analyses have been used to examine the synthesis of zeolite LTA and associated phases from metakaolinite. However, the synthesis product was controlled by the experimental method, taking into account that the classic hydrothermal transformation of the starting material produced a mixture of different zeolite-type structures, whereas the alkaline fusion approach promoted the crystallization of pure zeolite LTA.

----- **Keywords:** synthesis, metakaolinite, zeolite LTA, hydrothermal, crystallization

Resumen

La síntesis de zeolita LTA y fases asociadas a partir de metacaolinita se evaluaron mediante análisis de difracción de rayos X, microscopía electrónica de barrido, espectroscopia de infrarrojo por transformada de Fourier, resonancia magnética nuclear de ²⁹Si y ²⁷Al y análisis termogravimétrico. Sin embargo, el producto sintetizado fue controlado por el método experimental, teniendo en cuenta que la transformación hidrotérmica del material de partida por el método clásico produjo una mezcla de diferentes estructuras

* Autor de correspondencia: teléfono: 57 + 7 + 634 34 57, fax: 57 + 7 + 634 34 57, correo electrónico: carios@uis.edu.co (C. Ríos)

tipo zeolita, mientras que la aproximación por el método de fusión alcalina promovió la cristalización de zeolita LTA pura.

----- *Palabras clave:* síntesis, metakaolinita, zeolita LTA, hidrotérmico, cristalización

Introduction

The synthesis of crystalline aluminosilicate zeolites can be carried out from clay minerals, such as kaolinite [1, 2]. Previous work has shown that the improvement of the properties of kaolinite by chemical methods is difficult due to its low reactivity. This clay mineral is not significantly affected by acid or alkaline treatments, even under strong conditions [3-5]. Therefore, it is usually used after calcination at temperatures between 550-950 °C [6] to obtain a more reactive phase (metakaolinite) under chemical treatments, with the loss of structural water with reorganization of the structure. Only a small part of AlO_6 octahedra is maintained, while the rest are transformed into much more reactive tetra- and penta-coordinated units [7]. The optimum conditions for obtaining a very reactive metakaolinite have been discussed by several authors who reported values between 600-800 °C [8-10]. Calcination at higher temperatures leads to the formation of mullite and cristobalite [7]. Several authors have reported the synthesis of metakaolinite-based zeolitic materials, including the zeolite LTA [11-14]. In this work, we investigate the transformation of metakaolinite into zeolite LTA by two different methods: (1) conventional hydrothermal synthesis and (2) alkaline fusion followed by hydrothermal reaction.

Experimental

Reagents

Metakaolinite was obtained from calcination of kaolinite-rich clay (distributed under the name Supreme Powder and supplied by ECC International) and then used as starting material for zeolite synthesis. Other reagents used in the activation of kaolinite were: sodium hydroxide, NaOH, as pellets (99.99%, Aldrich Chemical Company, Inc.) or powder (96%, BDH Laboratory

Supplies), precipitated SiO_2 (BDH Laboratory Supplies), structure directing agents (SDAs) such as Tetrapropylammonium bromide (TPAB) (Aldrich Chemical Company, Inc.) and Triethylamine (TEA) (BDH Laboratory Supplies) and distilled water using standard purification methods.

Synthesis of zeolite LTA

Zeolite synthesis was investigated by two routes: (1) conventional hydrothermal synthesis and (2) alkaline fusion prior to hydrothermal synthesis. During the first method (Table 1), a calculated amount of NaOH pellets was added to distilled water in reaction plastic beakers (150–250 ml) to prepare NaOH solutions, in which metakaolinite was added. To evaluate the influence of additives, we conducted hydrothermal treatments with aqueous NaOH and precipitated SiO_2 to increase the Si/Al ratio. The addition of reagents was carried out under stirring conditions until they dissolved to homogenize the reaction gels. In the second method (Table 2), an alkaline fusion step was introduced prior to hydrothermal treatment. Metakaolinite was dry mixed with NaOH powder and the resultant mixture was fused at 600 °C for 1 h. The fused product was ground in a mortar and then a calculated amount of this was added to distilled water under stirring conditions.

Crystallization was carried out by hydrothermal synthesis under static conditions in PTFE vessels of 65 ml at 100°C and in teflon lined stainless steel autoclaves of 20 ml at 200°C for several reaction times. Once the activation time was reached, the reactors were removed from the oven and quenched in cold water to stop the reaction. After hydrothermal treatment, the reaction mixtures were filtered and washed with distilled water to remove excess alkali until the pH of the filtrate became neutral. Then, the samples were oven dried at 80°C overnight. Hydrogel pH was measured before and after hydrothermal treatment.

Table 1 Synthesis conditions for the conversion of metakaolinite into zeolitic materials using the conventional hydrothermal synthesis

Test	Chemical reagents				L/S		Hydrothermal reaction		Molar gel composition	Zeolitic phases and other synthesis products
	H ₂ O (g)	NaOH (g)	SDA (g)	SiO ₂ (g)	MTK (g)	(ml/g)	T (°C)	t (h)		
1	18,00	0,96			2,67	7,10	100	22	Na ₂ O:Al ₂ O ₃ :2SiO ₂ :84.2H ₂ O	LTA, SOD, CAN
2	18,00	0,96			2,67	7,10	100	28	Na ₂ O:Al ₂ O ₃ :2SiO ₂ :84.2H ₂ O	LTA, SOD, CAN
3	18,00	0,96			2,67	7,10	100	52	Na ₂ O:Al ₂ O ₃ :2SiO ₂ :84.2H ₂ O	LTA, SOD, CAN
4	18,00	0,96		0,24	2,67	7,10	100	24	Na ₂ O:Al ₂ O ₃ :2.3SiO ₂ :84.2H ₂ O	LTA
5	18,00	0,96		0,24	2,67	7,10	100	48	Na ₂ O:Al ₂ O ₃ :2.3SiO ₂ :84.2H ₂ O	LTA
6	18,00	0,96		0,24	2,67	7,10	100	72	Na ₂ O:Al ₂ O ₃ :2.3SiO ₂ :84.2H ₂ O	LTA
7	18,00	0,96		0,24	2,67	7,10	100	96	Na ₂ O:Al ₂ O ₃ :2.3SiO ₂ :84.2H ₂ O	LTA
8	18,00	2,87		0,24	2,67	7,82	200	6	3Na ₂ O:Al ₂ O ₃ :2.3SiO ₂ :86.2H ₂ O	LTA, SOD, CAN, JBW, ANA
9	18,00	2,87		0,24	2,67	7,82	200	24	3Na ₂ O:Al ₂ O ₃ :2.3SiO ₂ :86.2H ₂ O	LTA, SOD, CAN, JBW, ANA
10	18,00	2,87		0,24	2,67	7,82	200	48	3Na ₂ O:Al ₂ O ₃ :2.3SiO ₂ :86.2H ₂ O	LTA, SOD, CAN, JBW, ANA
11	18,00	0,96	TPAB		2,67	7,10	100	22	Na ₂ O:Al ₂ O ₃ :2SiO ₂ :0.5TPAB:84.2H ₂ O	LTA, SOD, CAN
12	18,00	0,96	TPAB		2,67	7,10	100	28	Na ₂ O:Al ₂ O ₃ :2SiO ₂ :0.5TPAB:84.2H ₂ O	LTA, SOD, CAN
13	18,00	0,96	TPAB		2,67	7,10	100	52	Na ₂ O:Al ₂ O ₃ :2SiO ₂ :0.5TPAB:84.2H ₂ O	LTA, SOD, CAN
14	18,00	0,96	TEA		2,67	7,10	100	24	Na ₂ O:Al ₂ O ₃ :2SiO ₂ :0.5TEA:84.2H ₂ O	LTA, SOD, CAN
15	18,00	0,96	TEA		2,67	7,10	100	48	Na ₂ O:Al ₂ O ₃ :2SiO ₂ :0.5TEA:84.2H ₂ O	LTA, SOD, CAN
16	18,00	0,96	TEA		2,67	7,10	100	72	Na ₂ O:Al ₂ O ₃ :2SiO ₂ :0.5TEA:84.2H ₂ O	LTA, SOD, CAN
17	18,00	0,96	TEA		2,67	7,10	100	24	Na ₂ O:Al ₂ O ₃ :2SiO ₂ :TEA:84.2H ₂ O	LTA, SOD, CAN
18	18,00	0,96	TEA		2,67	7,10	100	48	Na ₂ O:Al ₂ O ₃ :2SiO ₂ :TEA:84.2H ₂ O	LTA, SOD, CAN
19	18,00	0,96	TEA		2,67	7,10	100	72	Na ₂ O:Al ₂ O ₃ :2SiO ₂ :TEA:84.2H ₂ O	LTA, SOD, CAN

LTA, zeolite LTA; SOD, sodalite; CAN, cancrinite; JBW, zeolite JBW; ANA, analcime; L/S, activator solution/metakaolinite ratio; SDA, structure directing agent;

TPAB, tetrapropylammonium bromide; TEA, Triethylamine.

Table 2 Synthesis conditions for the conversion of metakaolinite into zeolitic materials using the alkaline fusion method

Test	Chemical reagents to be fused			Alkaline fusion		L/FP		Aging		Hydrothermal reaction		Molar gel composition		Zeolitic phases and other synthesis products
	MTK (g)	NaOH (g)	T (°C)	t (h)	T (°C)	t (h)	(ml/g)	t (h)	T (°C)	T (°C)	t (h)			
20	6,20	7,44	600	1	600	5.5 ^s	4,9	5.5 ^s	60	60	24	3.3Na ₂ O:Al ₂ O ₃ :2SiO ₂ :130.7H ₂ O		LTA
21	6,20	7,44	600	1	600	5.5 ^s	4,9	5.5 ^s	60	60	48	3.3Na ₂ O:Al ₂ O ₃ :2SiO ₂ :130.7H ₂ O		LTA
22	6,20	7,44	600	1	600	5.5 ^s	4,9	5.5 ^s	60	60	96	3.3Na ₂ O:Al ₂ O ₃ :2SiO ₂ :130.7H ₂ O		LTA

LTA, zeolite LTA; L/FP, water/fused product ratio; ^sstirring conditions.

Characterization techniques

XRD patterns of the untreated kaolinite and synthesis products were recorded using a Philips PW1710 diffractometer operating in Bragg-Brentano geometry with Cu-K α radiation (40 kV and 40 mA) and secondary monochromation. Data collection was carried out in the 2θ range 3-50°, with a step size of 0.02°. Phase identification was performed by searching the ICDD powder diffraction file database, with the help of JCPDS files for inorganic compounds. The morphology of the solid phases were examined by scanning electron microscopy (ZEISS EVO50) under the following analytical conditions: I probe 1 nA, EHT = 20.00 kV, beam current 100 μ A, Signal A = SE1, WD = 8.0 mm. Fourier transform infrared (FTIR) spectroscopy was carried out using a Mattson Genesis II FT-IR spectrometer in the 4000-400 cm⁻¹ region. Nuclear magnetic resonance spectra for ²⁹Si, ²⁷Al were recorded on a Varian UnityInova spectrometer under the following analytical conditions: MAS probe 7.5-4.0 mm; frequency 59.6-78.1 MHz; spectral width 29996-100000 Hz; acquisition time 30-10 ms; recycle time 120-0.5 s; number of repetitions 15-2200; spinning rate 5040-14000 Hz; pulse angle $\pi/2-\pi/10$. The chemical shifts were referenced to tetramethylsilane (TMS) for ²⁹Si and 1 M AlCl₃ aqueous solution for ²⁷Al. Thermogravimetric analyses were performed on a Mettler Toledo TG 50 thermobalance. Samples ~15-20 mg were heated under nitrogen gas flow (20 mL/min) between 25-700 °C at a rate of 20 °C/min.

Results and discussion

Characterization of the unreacted and thermally treated kaolinite

XRD patterns of the untreated and thermally treated kaolinite are shown in figure 1. Metakaolinite is characterized by the disappearance of all the XRD peaks of kaolinite, accompanied by the appearance of an amorphous aluminosilicate (see the broad hump at $2\theta = 13-33^\circ$). However, metakaolinite contains mullite as the main

crystalline phase at 1000 °C. Therefore, MTK600 was used as starting material in zeolite synthesis. Similar results have reported by Mackenzie [6] for calcination at higher temperatures, which leads to the formation of mullite and cristobalite. After the decomposition of kaolinite, the higher-order reflections of this mineral lost their intensity and merged into the XRD background, which led to the opinion that metakaolinite can be amorphous, although actually a conception of the short-range order crystalline structure of metakaolinite predominates [15].

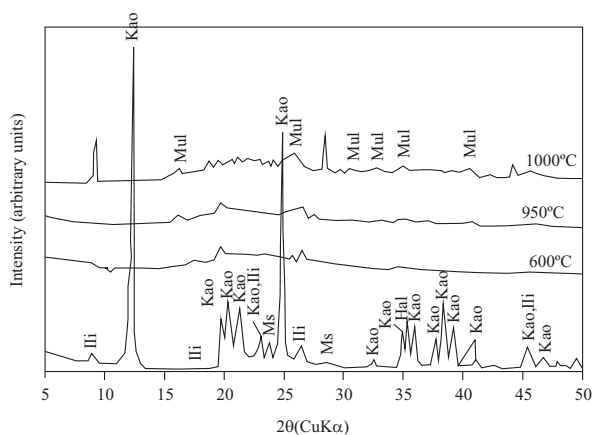


Figure 1 X-ray diffraction patterns of unreacted (background) and thermally treated kaolinite at different temperatures. Ili, illite; Kao, kaolinite; Ms, muscovite; Hal, halloysite; Mul, mullite

Figure 2 illustrates the FT-IR spectra over the range 400–4000 cm^{-1} , corresponding to the transformation of kaolinite-rich clay to metakaolinite. The bands at 3692 and 3619 cm^{-1} are assigned to the stretching vibration of hydroxyl groups of kaolinite [16–19]. However, the bands at 3669 and 3652 cm^{-1} reported in a previous work [18] were not observed. The band at 3692 cm^{-1} represents the stretching vibration modes of ‘inner surface hydroxyls’ that are located at the surface of octahedral sheets opposite to the tetrahedral oxygens of the adjacent kaolinite layer, whereas the band at 3619 cm^{-1} is related to the stretching vibration modes of ‘inner hydroxyls’ and refers to OH groups located in the plane

common to octahedral and tetrahedral sheets [20]. The band at 1119 cm^{-1} is referred to Si-O stretching vibrations, while the bands at 1034 and 1012 cm^{-1} are rather caused by Si-O-Si and Si-O-Al lattice vibrations [21]. The OH bending vibrations at 942 and 916 cm^{-1} are referred to the ‘surface OH bending’ and ‘inner OH bending’ [22]. Further, bands at 762, 696 and 539 cm^{-1} can be largely attributed to different Si-O and Al-O vibrations; the first two of them are attributed to the distortion of the tetrahedral and octahedral layers [23]. The transformation of kaolinite to metakaolinite is revealed by the disappearance of the characteristic bands of kaolinite. These changes are similar to those reported in other studies [24, 25]. The characteristic bands observed in metakaolinite were 1049, 802, 642, 571 and 434 cm^{-1} , with three broad bands centred at 1049, 802 and 434 cm^{-1} . A significant shift of the Si-O vibration bands at 1034 and 1012 cm^{-1} in kaolinite to a higher frequency band at 1049 cm^{-1} in metakaolinite was observed, which is attributed to amorphous SiO_2 [26–28]. The stretching vibration of Al (O,OH)₆ octahedra in kaolinite [7] is observed at 539 cm^{-1} , but is substituted by a peak at 802 cm^{-1} corresponding to the vibration band of AlO_4 tetrahedron in metakaolinite. The splitting of the 802 cm^{-1} band into two separate modes at 784 and 811 cm^{-1} with increasing temperature, which is attributed to the formation of mullite from Al–Si-spinel.

The ^{29}Si and ^{27}Al NMR spectra of the untreated and treated kaolinite are given in figure 3. ^{29}Si NMR spectrum of kaolinite (figure 3a) displays two well resolved signals at -90.9 and -91.4 ppm attributed to the existence of two different but equally populated silicon sites. The observation of these different ^{29}Si NMR signals for kaolinite was reported previously [29, 30]. Interlayer hydrogen bonding resulting in two different silicon environments is the main reason for the ^{29}Si NMR signal splitting in kaolinite [31]. ^{29}Si NMR spectrum of metakaolinite (figure 3b) displays a broad signal around -96.3 ppm attributed to Si linked to four other Si atoms in silica polymorphs [32], and the presence of amorphous silica [33]. Previous

studies have examined these signals in detail [34, 35]. When kaolinite is dehydroxylated, the Si atoms undergo a range of environments of different distortion and the broadness of the metakaolinite line is attributed to these variations in the Si-O-Si(Al) bond angles [36]. The ^{27}Al NMR spectrum of kaolinite (figure 3a) consists of a single resonance at -3.4 ppm assigned to 6-coordinated Al. The dehydroxylation of kaolinite brings about major changes, especially in the octahedral Al-O layers which are most closely associated with the structural hydroxyl groups [36]. This is graphically illustrated by the change in the ^{27}Al NMR spectrum from a sharp octahedral Al-O resonance in kaolinite to a spectrum containing broad overlapping resonances at -0.3, 23.4 and 45.9 ppm (figure 3b) attributed to 6-, 5- and 4-coordinated Al local environments [37]. The broader and asymmetrical peak shapes of metakaolinite show its disordered structure [16].

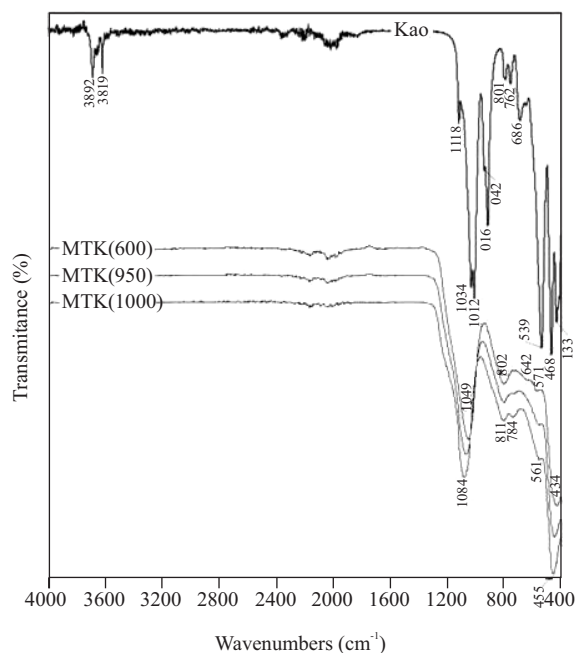


Figure 2 FT-IR spectra of the kaolinite-rich clay and its calcination product (metakaolinite) obtained at 600, 950 and 1000 °C

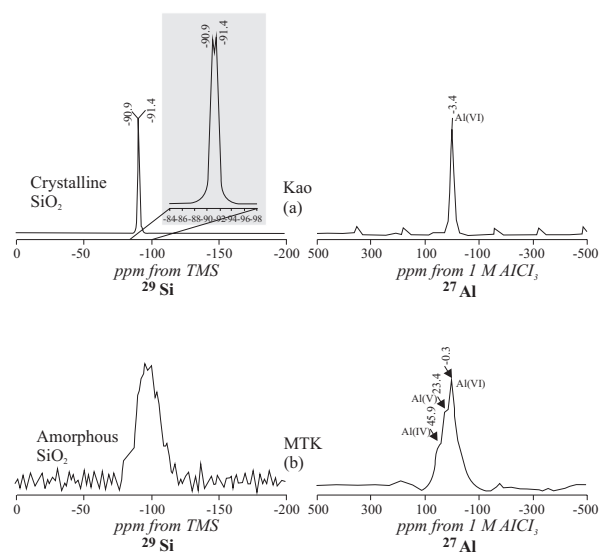


Figure 3 ^{29}Si and ^{27}Al NMR spectra of (a) kaolinite and (b) metakaolinite

Characterization of metakaolinite-based zeolites

X-ray diffraction analysis

Figure 4 shows the XRD patterns of metakaolinite and synthesis products after its hydrothermal reaction with alkaline solutions. The most important change observed is the appearance of the characteristic peaks of zeolite LTA, sodalite and cancrinite with traces of zeolite JBW and analcime. The as-synthesized zeolite LTA has several common peaks on its XRD pattern (figure 4a). Figure 4b indicates that when precipitated SiO_2 was used at low temperature and NaOH concentration, the synthesis product is characterized by peaks corresponding to zeolite LTA at shorter reaction time (24 h), which tend to be constant, and disappear with reaction time to produce an amorphous aluminosilicate material (96 h). On the other hand, the addition of precipitated SiO_2 at high temperature and NaOH concentration (figure 4c) produced a mixture of zeolite LTA, sodalite, cancrinite, zeolite JBW and analcime, which show similar crystallinity during the monitoring time. As occurred with kaolinite, the use of SDAs produced a reduction

in the intensity of the peaks of zeolite LTA and associated phases (figures 4d and 4e). Figure 4f shows the XRD patterns of the treated

metakaolinite following the fusion approach, which indicates that only zeolite LTA crystallized in spite of the hydrothermal reaction time.

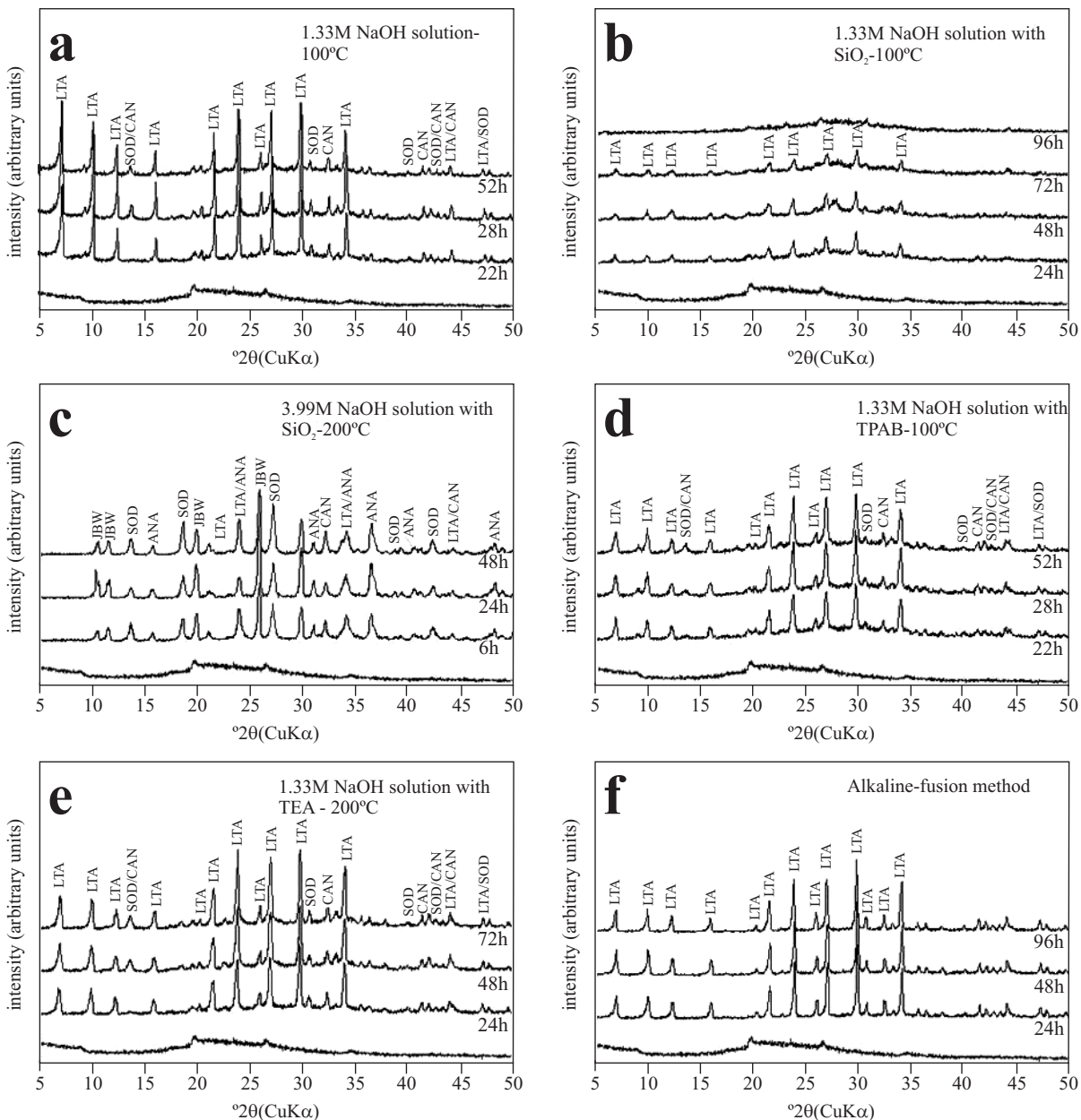


Figure 4 X-ray diffraction patterns of the unreacted (background) metakaolinite and representative as-synthesized products obtained via (a-e) hydrothermal reaction of metakaolinite in NaOH solutions with addition of organic templates or SiO₂ and (f) alkaline fusion method

Scanning electron microscopy

SEM images in figure 5 illustrate several aspects on the occurrence of representative as-synthesized products obtained using metakaolinite as a starting material, with cubic crystals of zeolite LTA as the main synthesis product. Lepispheric morphologies corresponding to sodalite and cancrinite grow at the surface of cubic crystals of zeolite LTA (figure 5a), which sometimes display interpenetrating twinning, at 1.33M NaOH solutions at 100 °C for 52 h. Some deformed pseudo-hexagonal platelets of the original kaolinite still remain after its activation. When metakaolinite was treated at low NaOH concentration and temperature with the addition of precipitated SiO₂, amorphous spheroidal morphologies, from which relicts of unreacted metakaolinite (morphology showing

distorted pseudo-hexagonal platelets) can be observed in a radial arrangement (figure 5b). At higher NaOH concentration and temperature, a co-crystallization of sodalite and cancrinite was followed by zeolite JBW formation (figure 5c). A similar relationship, describing a phase transformation from zeolite LTA to zeolite JBW, has been described in a previous study [38]. However, in this study is suggested a phase transformation from metastable zeolite LTA to sodalite and cancrinite prior to zeolite JBW formation. Figure 5d shows the occurrence of zeolite LTA obtained by alkaline fusion of metakaolinite followed by hydrothermal reaction, displaying a cubic morphology with varying expression of facets and surface terraces, and occasionally intergrown twins with a particle size of 1 μm (average).

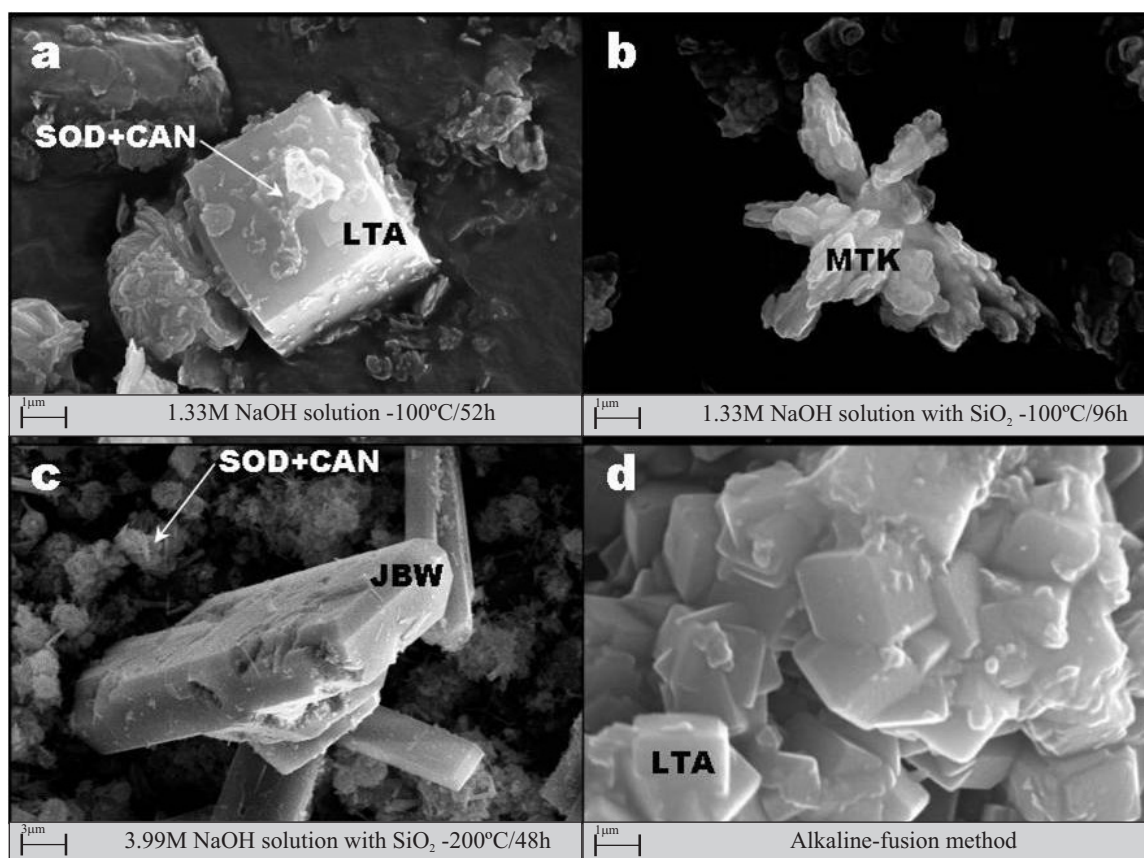


Figure 5 SEM micrographs showing the occurrence of representative as-synthesized products obtained via (a-c) hydrothermal reaction of metakaolinite in NaOH solutions and (d) alkaline fusion method with NaOH as an activator agent

Fourier transform infrared spectroscopy

Figure 6 illustrates the FT-IR spectra of the unreacted and reacted metakaolinite. The characteristic vibration bands of metakaolinite disappeared, accompanied by the appearance of new peaks revealing the occurrence of zeolite LTA. The band at 1047 cm⁻¹ shifted to lower frequency bands (at 973-980 cm⁻¹); the band at 800 cm⁻¹ disappeared in the synthesis products; the low intensity bands at 635 and 565 cm⁻¹ shifted to higher (at 673-690 cm⁻¹) and lower (at 530-538 cm⁻¹) frequency bands, respectively. The band at 424 cm⁻¹ shifted to lower frequency bands (at

411-417 cm⁻¹). The typical bands of zeolite LTA are represented by asymmetric Al-O (973-980 cm⁻¹) and symmetric Al-O (673-690 cm⁻¹) stretches, and double rings (530-538 cm⁻¹). The activation of metakaolinite resulted in a shift to lower wavenumbers, revealing more Al substitution in tetrahedral sites. The alkaline fusion approach produced zeolite LTA, which shows a well-defined FT-IR spectra, with sharp peaks centred at 549-551 and 463-464 cm⁻¹, which reveals a pure synthesis product with higher crystallinity. On the other hand, this can also be attributed to the occurrence of better defined structures (zeolite LTA) containing more Al in tetrahedral coordination.

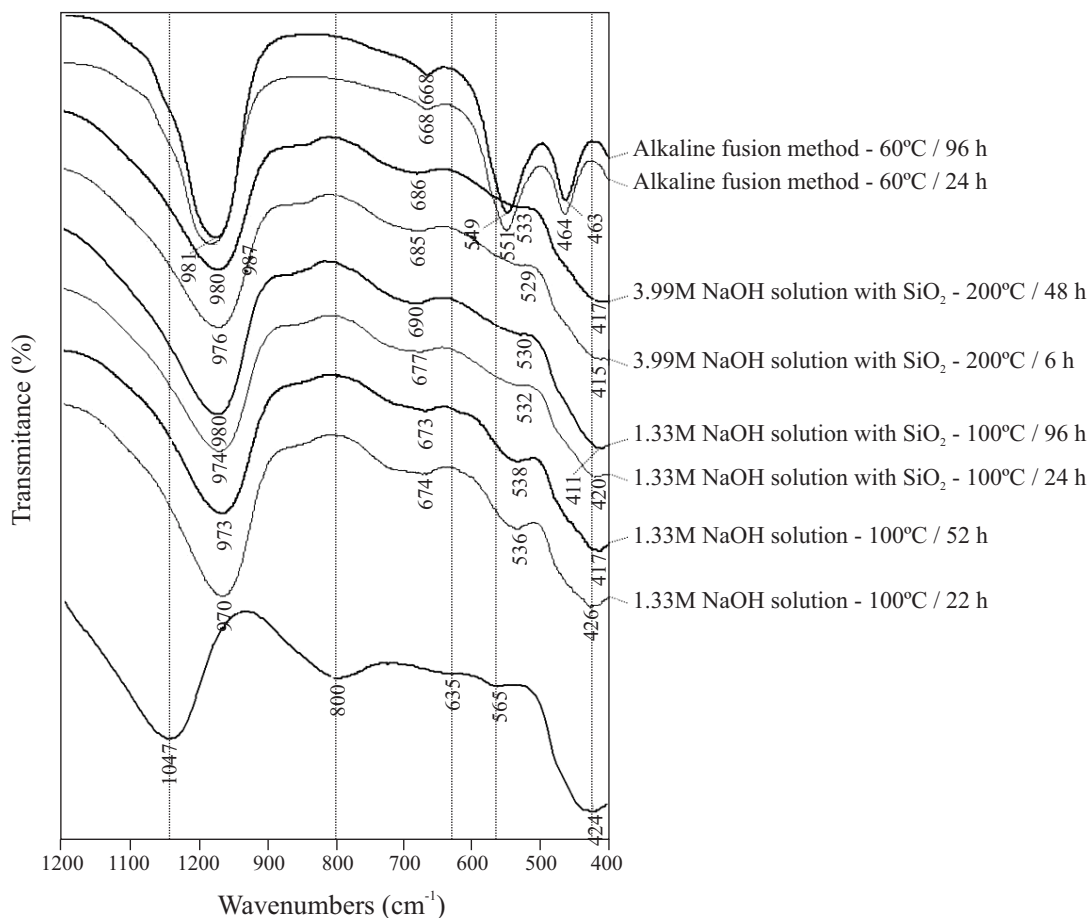


Figure 6 FT-IR spectra of the unreacted (background) metakaolinite and representative as-synthesized products obtained after its alkaline activation using NaOH activator agent

^{29}Si and ^{27}Al nuclear magnetic resonance

Figure 7 shows the ^{29}Si and ^{27}Al NMR spectra of the metakaolinite and representative synthesis products. ^{29}Si NMR spectrum of metakaolinite (figure 7a) shows a broad single resonance centred at -96.3 ppm, attributed to a range of Q^4 environments. Figure 7b shows a sharp ^{29}Si signal at -89.5 ppm, which is characteristic of $\text{Q}^4(4\text{Al})$ sites in zeolite LTA, similar to what is reported in previous studies [24]. A weak signal at -85.9 ppm is attributed to the contribution of $\text{Q}^4(4\text{Al})$ sites of sodalite and cancrinite. ^{29}Si NMR points out the change of the silica morphology from amorphous SiO_2 in metakaolinite to crystalline SiO_2 in metakaolinite-based aluminosilicates, with the total dissolution of the starting metakaolinite to form zeolite-type structures and the incorporation of Al. ^{27}Al NMR spectrum of metakaolinite (figure 7b) shows two resonances at -0.3 and 23.4 ppm can be attributed to 6- and 5-coordinated Al. Figure 7b shows a single resonance at 58.2 ppm, attributed to tetrahedral Al in the synthesis product.

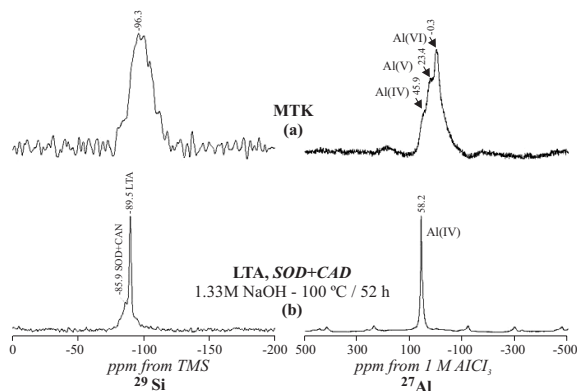


Figure 7 ^{29}Si and ^{27}Al NMR spectra of the (a) metakaolinite and (b) representative synthesis products obtained after hydrothermal reaction of metakaolinite with NaOH activator agent

Thermogravimetric analyses

DTG curves of the metakaolinite-based zeolitic materials are shown in figure 8. The as-synthesized products generally show two dehydration steps. The peaks observed between 39-52 °C correspond

to surface water in zeolitic materials; the peaks observed between 100-162 °C indicate zeolitic water, although in some cases in this temperature range up to two peaks occur, which can be explained by the heterogeneous nature of the as-synthesized products. The synthetic zeolitic products obtained after hydrothermal transformation of metakaolinite in solutions of 1.33M NaOH at 100 °C for 52 h shows the highest weight loss (19.48%).

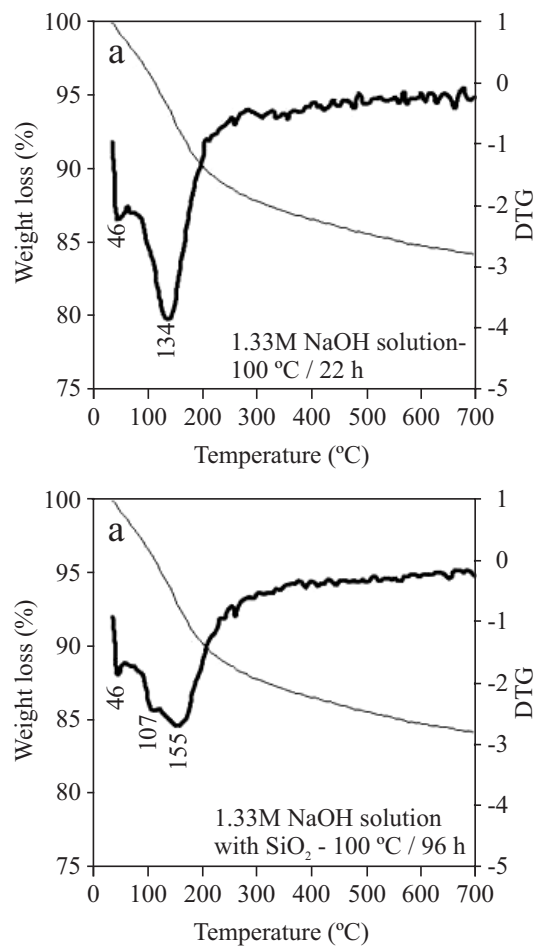


Figure 8 TG/DTG curves between 25 and 700 °C of representative synthesis products obtained after alkaline activation of metakaolinite using NaOH as activator agent

Conclusions

Zeolite LTA was successfully synthesized after alkaline hydrothermal treatment of metakaolinite. However, the synthesis product was controlled

by the experimental method, taking into account that the classic hydrothermal transformation of metakaolinite produced a mixture of different zeolite-type structures, whereas the alkaline fusion approach promoted the crystallization of pure zeolite LTA. The addition of precipitated SiO₂ at low NaOH concentrations and temperature produced only zeolite LTA, although with a constant low grade of crystallinity and the presence of an amorphous aluminosilicate phase at longer reaction times. However, using this silica source at high NaOH concentrations and temperature, several crystallinity phases (zeolite LTA, sodalite, cancrinite, zeolite JBW and analcime) were obtained. The use of SDAs produced a reduction in the intensity of the peaks of zeolite LTA and associated phases. The alkaline activation of metakaolinite following the fusion approach favoured the crystallization of pure zeolite LTA stable for 96 h of monitoring time. This synthesis product is characterized by a high grade of crystallinity and uniform crystal size distribution (1.0 µm).

Acknowledgments

We gratefully acknowledge the European Union Programme of High Level Scholarships for Latin America, scholarship No. E05D060429CO, and the Universidad Industrial de Santander for funding C. A. Ríos. Special thanks to the School of Applied Sciences of the University of Wolverhampton for allowing us the use of the research facilities. We thank to D. Townrow and B. Hodson for assistance in collecting XRD and SEM data, respectively, and to D. Apperley and the EPSRC solid state NMR Service of the University of Durham for NMR spectra.

References

1. D. Boukadir, N. Bettahar, Z. Derriche. "Synthesis of zeolites 4A and HS from natural materials". *Annales de Chimie - Science des Matériaux*. Vol. 27. 2002. pp. 1-13.
2. C. A. Ríos, C. D. Williams, M. A. Fullen. "Nucleation and growth history of zeolite LTA synthesized from kaolinite by two different methods". *Applied Clay Science*. Vol. 42. 2009. pp. 446-454.
3. R. Lussier. A novel clay-based catalytic material-preparation and properties. *Journal of Catalysis*. Vol. 129. 1991. pp. 225-237.
4. M. Perissinotto, L. Storaro, M. Lenarda, R. J. Ganzerla. "Solid acid catalysts from clays: Acid leached metakaolin as isopropanol". *Journal of Molecular Catalysis A: Chemistry*. Vol. 121. 1997. pp. 103-109.
5. A. Demortier, N. Gobeltz, J. P. Lelieur, C. Duhayon. "Infrared evidence for the formation of an intermediate compound during the synthesis of zeolite Na-A from metakaolin". *International Journal of Inorganic Materials*. Vol. 1. 1999. pp. 129-134.
6. R. C. Mackenzie. *Differential Thermal Analysis I*. Academic Press. London. 1970. pp. 504-514.
7. J. F. Lambert, W. S. Minman, J. J. Fripiat. "Revisiting kaolinite dehydroxylation: A silicon-29 and aluminum-27 MAS NMR study". *Journal of American Chemistry Society*. Vol. 111. 1989. pp. 517-522.
8. M. Murat, A. Amorkrane, J. P. Bastide, L. Montanaro. "Synthesis of zeolites from thermally activated kaolinite. Some observations on nucleation and growth". *Clay Minerals*. Vol. 27. 1992. pp. 119-130.
9. S. Chandrasekhar, P. N. Pramada. "Investigation on the synthesis of zeolite NaX from Kerala kaolin". *Journal of Porous Materials*. Vol. 6. 1999. pp. 283-297.
10. M. Xu, M. Cheng, X. Bao, X. Liu, D. Tang. "Growth of zeolite KSO1 on calcined kaolin microspheres". *Journal of Material Chemistry*. Vol. 9. 1999. pp. 2965-2966.
11. J. Rocha, J. Klinowski, J. M. Adams. "Synthesis of zeolite Na-A from metakaolinite revisited". *Journal of the Chemical Society Faraday Transactions*. Vol. 87. 1991. pp. 3091-3097.
12. I. Lapidés, L. Heller-Kallai. "Reactions of metakaolinite with NaOH and colloidal silica - Comparison of different samples (Part 2)". *Applied Clay Science*. Vol. 35. 2007. pp. 94-98.
13. L. Heller-Kallai, I. Lapidés. "Reactions of kaolinites and metakaolinites with NaOH - comparison of different samples (Part 1)". *Applied Clay Science*. Vol. 35. 2007. pp. 99-107.
14. C. A. Ríos, C. D. Williams, M. J. Maple. "Synthesis of zeolites and zeotypes by hydrothermal transformation of kaolinite and metakaolinite". *Bistua*. Vol. 5. 2007. pp. 15-26.
15. S. Lee, Y. J. Kim, H. S. Moon. "Energy-filtering electron microscopy (EF-TEM) study of a modulated structure in metakaolinite represented by a 14 modulation". *Journal of American Ceramic Society*. Vol. 86. 2003. pp. 174-176.

16. Q. Liu, D. A. Spears, Q. Liu. "MAS NMR study of surface-modified calcined kaolin". *Applied Clay Science*. Vol. 19. 2001. pp. 89-94.
17. N. J. Saikia, D. J. Bharali, P. Sengupta, D. Bordoloi, R. L. Goswamee, P. C. Saikia, P. C. Bothakur. "Characterization, beneficiation and utilization of kaolinite clay from Assam". *Indian Applied Clay Science*. Vol. 24. 2003. pp. 93-103.
18. H. Zhao, Y. Deng, J. B. Harsh, M. Flury, J. S. Boyle. "Alteration of kaolinite to cancrinite and sodalite by simulated hanford tank waste and its impact on cesium retention". *Clays and Clay Minerals*. Vol. 52. 2004. pp. 1-13.
19. M. Alkan, C. Hopa, Z. Yilmaz, H. Guler. "The effect of alkali concentration and solid/liquid ratio on the hydrothermal synthesis of zeolite NaA from natural kaolinite". *Microporous and Mesoporous Materials*. Vol. 86. 2005. pp. 176-184.
20. J. Kristof, J. Mink, E. Horvath, M. Gabor. "Intercalation study of clay minerals by Fourier transform infrared spectrometry". *Vibrational Spectroscopy*. Vol. 5. 1993. pp. 61-67.
21. R. G. Worln. "Structural aspects of kaolinite using infrared absorption". *The American Mineralogist*. Vol. 48. 1963. pp. 390-399.
22. R. L. Frostm, E. Mako, J. Krsitof, J. T. Klopogge. "Modification of kaolinite surfaces through mechanochemical treatment - a mid-IR and near-IR spectroscopic study". *Spectrochimica Acta Part A: Molecular and Biomolecular Spectroscopy*. Vol. 58. 2002. pp. 2849-2859.
23. M. Hoch, A. Bandara. "Determination of the adsorption process of tributyltin (TBT) and monobutyltin (MBT) onto kaolinite surface using Fourier transform infrared (FTIR) spectroscopy". *Colloids and Surfaces A: Physicochemical and Engineering Aspects*. Vol. 253. 2005. pp. 117-124.
24. D. Akolekar, A. Chaffee, R. F. Howe. "The transformation of kaolin to low-silica X zeolite". *Zeolites*. Vol. 19. 1997. pp. 359-365.
25. C. Covarrubias, R. García, R. Arriagada, J. Yanez, T. Garland. "Cr(III) exchange on zeolites obtained from kaolin and natural mordenite". *Microporous and Mesoporous Materials*. Vol. 88. 2006. pp. 220-231.
26. P. K. Sinha, P. K. Paniker, R. V. Amalraj. "Treatment of radioactive liquid waste containing caesium by indigenously available synthetic zeolites: A comparative study". *Waste Management*. Vol. 15. 1995. pp. 149-157.
27. E. Valcke, B. Engels, A. Cremers. "The use of zeolites as amendments in radiocaesium- and radiostromtium-contaminated soils: A soil-chemical approach. Part II: Sr-Ca exchange in clinoptilolite, mordenite and zeolite A". *Zeolites*. Vol. 18. 1997. pp. 212-217.
28. G. Qiu, T. Jiang, G. Li, X. Fan, Z. Huang. "Activation and removal of silicon in kaolinite by thermochemical process". *Scandinavian Journal of Metallurgy*. Vol. 33. 2004. pp. 121-128.
29. P. F. Barron, R. L. Frost, J. O. Skjemstad, A. J. Koppi. "Detection of two silicon environments in kaolins by solid-state silicon-29 NMR". *Nature*. Vol. 302. 1983. pp. 49-50.
30. S. Letaief, T. A. Elbokl, C. Detellier. "Reactivity of ionic liquids with kaolinite: Melt intersalation of ethyl pyridinium chloride in an urea-kaolinite pre-intercalate". *Journal of Colloid and Interface Science*. Vol. 302. 2006. pp. 254-258.
31. J. G. Thompson, P. F. Barron. "Further consideration of the ²⁹Si nuclear magnetic resonance spectrum of kaolinite". *Clays and Clay Minerals*. Vol. 35. 1987. pp. 38-42.
32. J. V. Smith, C. S. Blackwell. "Nuclear magnetic resonance of silica polymorphs". *Nature*. Vol. 303. 1983. pp. 223-225.
33. J. Rocha, J. Klinowski. "²⁹Si and ²⁷Al magic-angle-spinning MAS NMR studies of the thermal transformation of kaolinite". *Journal of Physics and Chemistry of Minerals*. Vol. 17. 1990. pp. 179-186.
34. A. Madani, A. Aznar, J. Sanza, J. M. Serratosa. "Si and Al MAS NMR study of zeolite formation from alkali-leached kaolinites. Influence of thermal activation". *Journal of Physics and Chemistry B*. Vol. 94. 1990. pp. 760-765.
35. A. Palomo, S. Alonso, A. Fernández-Jiménez, I. Sobrados, J. Sanz. "Alkaline activation of fly ashes. A ²⁹Si MAS NMR study of the reaction products". *Journal of American Ceramic Society*. Vol. 87. 2004. pp. 1141-1145.
36. K. J. D. Mackenzie, I. W. M. Brown, R. H. Meinhold, M. E. Bowden. "Outstanding problems in the kaolinite-mullite reaction sequence investigated by ²⁹Si and ²⁷Al Solid-State Nuclear Magnetic Resonance: I. Metakaolinite". *Journal of American Ceramic Society*. Vol. 68. 1985. pp. 293-297.
37. R. Rocha. "Single- and triple-quantum ²⁷Al MAS NMR study of the thermal transformation of kaolinite". *Journal of Physics and Chemistry B*. Vol. 103. 1999. pp. 9801-9804.
38. D. C. Lin, X. W. Xu, F. Zuo, Y. C. Long. "Crystallization of JBW, CAN, SOD and ABW type zeolite from transformation of metakaolin". *Microporous and Mesoporous Materials*. Vol. 70. 2004. pp. 63-70.